The PARP inhibitor olaparib induces significant killing of *ATM*-deficient lymphoid tumor cells in vitro and in vivo

*Victoria J. Weston,[1] *Ceri E. Oldreive,[1] Anna Skowronska,[1] David G. Oscier,[2] Guy Pratt,[3] Martin J. S. Dyer,[4] Graeme Smith,[5] Judy E. Powell,[6] Zbigniew Rudzki,[7] Pamela Kearns,[1] Paul A. H. Moss,[1] A. Malcolm R. Taylor,[1] and Tatjana Stankovic[1]

[1]School of Cancer Sciences, University of Birmingham, Birmingham, United Kingdom; [2]Haematology Department, Royal Bournemouth Hospital, Dorset, United Kingdom; [3]Haematology Department, Heartlands Hospital, Birmingham, United Kingdom; [4]Medical Research Council (MRC) Toxicology Unit, Leicester University, Leicester, United Kingdom; [5]AstraZeneca Pharmaceuticals, Cambridge, United Kingdom; [6]School of Health and Population Sciences, University of Birmingham, Birmingham, United Kingdom; and [7]Pathology Department, Heartlands Hospital, Birmingham, United Kingdom

The *Ataxia Telangiectasia Mutated (ATM)* gene is frequently inactivated in lymphoid malignancies such as chronic lymphocytic leukemia (CLL), T-prolymphocytic leukemia (T-PLL), and mantle cell lymphoma (MCL) and is associated with defective apoptosis in response to alkylating agents and purine analogues. *ATM* mutant cells exhibit impaired DNA double strand break repair. Poly (ADP-ribose) polymerase (PARP) inhibition that imposes the requirement for DNA double strand break repair should selectively sensitize ATM-deficient tumor cells to killing. We investigated in vitro sensitivity to the poly (ADP-ribose) polymerase inhibitor olaparib (AZD2281) of 5 *ATM* mutant lymphoblastoid cell lines (LCL), an *ATM* mutant MCL cell line, an *ATM* knockdown PGA CLL cell line, and 9 *ATM*-deficient primary CLLs induced to cycle and observed differential killing compared with *ATM* wildtype counterparts. Pharmacologic inhibition of ATM and *ATM* knockdown confirmed the effect was ATM-dependent and mediated through mitotic catastrophe independently of apoptosis. A nonobese diabetic/severe combined immunodeficient (NOD/SCID) murine xenograft model of an *ATM* mutant MCL cell line demonstrated significantly reduced tumor load and an increased survival of animals after olaparib treatment in vivo. Addition of olaparib sensitized *ATM* null tumor cells to DNA-damaging agents. We suggest that olaparib would be an appropriate agent for treating refractory *ATM* mutant lymphoid tumors. (*Blood*. 2010; 116(22):4578-4587)

Introduction

The *Ataxia Telangiectasia Mutated* (*ATM*) tumor suppressor gene encodes a principal DNA damage–signaling protein, and cells with ATM dysfunction exhibit increased radiosensitivity, loss of cell-cycle checkpoints, and p53 dysfunction.[1-5] In addition to the impaired apoptotic response, the cellular phenotype of these cells can be attributed to subtle but significant defects in both major types of DNA double strand break (DSB) repair: error-prone non-homologous end joining (NHEJ), preferentially employed in the gap 1 (G1) phase of the cell cycle, and error-free homologous recombination (HR) repair, restricted to synthesis/gap 2/mitosis (S/G2/M) phases of the cell cycle.[6-11] After DNA damage, *ATM* mutant cells consequently exhibit prolonged DNA DSBs and abnormal retention of DNA proteins at the sites of DNA DSB observed as intra-nuclear foci.[6-11]

Inactivation of *ATM* is a frequent event in lymphoid malignancies such as B-cell chronic lymphocytic leukemia (CLL),[12-14] T-prolymphocytic leukemia (T-PLL)[15,16] and mantle cell leukemia (MCL).[17] CLL is the most common leukemia in western countries. While many patients do not require therapeutic intervention, those with progressive CLL have a poor overall outcome, and survival is greatly impaired by the presence of genetic abnormalities such as 11q deletions/*ATM* mutations and 17p deletions/*TP53* mutations.[18-23] The less-frequent malignancies, T-PLL and MCL, also commonly harbor 11q deletions and *ATM* mutations,[15-17] which may contribute to their dismal clinical responses. Progressive lymphoid malignancies are currently treated with combinations of nucleoside analogues and alkylating agents, which typically exert their effect through the generation of DNA damage and subsequent induction of an ATM/p53-dependent apoptotic pathway.[24] Consistent with this mechanism, ATM mutant CLL cells exhibit resistance to fludarabine-induced apoptosis in vitro.[21] The adverse impact of *ATM* inactivation on clinical responses of this subtype to current therapies may be evident at several levels: The presence of pathogenic *ATM* mutations causes rapid clonal expansion of 11qdel subclones[21] and significantly reduces overall survival[21] as well as progression-free survival in patients treated in the United Kingdom CLL4 trial (A.S., V.W., D.O., G.P., A.M.R.T., T.S., manuscript in preparation). Recent developments in front-line regimens by the addition of rituximab to fludarabine and cyclophosphamide (FCR) and second-line alemtuzumab and flavopiridol[22-27] has resulted in some clinical benefits for 11q del CLL[24] as well as other progressive lymphomas.[26,27] Despite these improvements, immunosuppression and toxicity associated with these new first- and second-line agents emphasizes the requirement for the identification of novel targeted drugs for the treatment of chemoresistant *ATM* mutant lymphoid tumors.

A favorable approach to designing targeted therapy is either to undermine redundant pathways or enhance deficiencies, already

Submitted January 20, 2010; accepted August 2, 2010. Prepublished online as *Blood* First Edition paper, August 25, 2010; DOI 10.1182/blood-2010-01-265769.

*V.J.W. and C.E.O. contributed equally to the manuscript.

The online version of this article contains a data supplement.

The publication costs of this article were defrayed in part by page charge payment. Therefore, and solely to indicate this fact, this article is hereby marked "advertisement" in accordance with 18 USC section 1734.

present in the cell, that are potentially lethal for the tumor. For example, a DNA repair inhibitor can facilitate conversion of one form of DNA damage into another form, which, in a cell with a particular mutated gene, cannot be repaired and leads to cell death.[28] This is the concept of synthetic lethality: when inactivation of either of 2 genes alone allows cell viability but simultaneous inactivation of both genes causes cell death.[28] Using this mechanism, poly (ADP-ribose) polymerase (PARP) inhibitors were recently shown to selectively target DNA DSB repair–deficient *BRCA1/2* null cells for killing.[29,30] After inhibition of PARP1, a component of the DNA single strand break (SSB) repair machinery,[29-31] unrepaired SSB lesions are converted into DNA DSBs during DNA replication and require activation of HR repair proteins (eg, BRCA1/2) for their resolution. Thus, *BRCA1/2* functionally null tumor cells treated with PARP inhibitor accumulate extensive DNA DSBs and undergo cellular death.[29-31] HR-impaired cells are, therefore, sensitive to PARP inhibition.[32]

ATM null cells show some deficiency in HR repair. Indeed, it has been shown in 2 independent studies that cells with ATM knockdown, like *BRCA1/2* null cells, also exhibit selective sensitivity to PARP inhibition.[33,34] In the present study we investigated whether the synthetic lethality resulting from PARP inhibitor treatment of *ATM* null cells[33,34] would also be applicable to *ATM* mutant lymphoid tumors and result in their specific killing. We have demonstrated a differential in vitro and in vivo sensitivity of primary and transformed *ATM* mutant CLL and MCL tumor cells to a new clinically tested PARP inhibitor, olaparib.[35,36]

Methods

Patients

CLL samples were obtained from Birmingham and Bournemouth Hospitals. Ethical approval was obtained from the South Birmingham Ethics Committee. A total of 17 CLLs with wildtype *ATM* and 14 CLL tumors with *ATM* dysfunction were used in the study, and their cellular features are given in supplemental Table 1 (available on the *Blood* Web site; see the Supplemental Materials link at the top of the online article).

Cell lines, retroviral *ATM* knockdown, and pharmacologic ATM inhibition

Lymphoblastoid cell lines (LCLs) generated from 5 healthy donors and 5 individuals with *ataxia-telangiectasia* (A-T), MCL cell lines with either a confirmed ATM defect (Granta-519) or functional ATM (JVM-2; supplemental Figure 1), and the CLL cell line, PGA[37] were employed. Stable knockdown in PGA cells was performed using RNA oligonucleotides (Dharmacon) targeting either green fluorescent protein (GFP) as a negative control (PGA-*GFP*sh) or *ATM* (PGA-*ATM*sh) as previously described.[38] Knockdown was shown to be stable by assessment of ATM activity through ionizing radiation (IR)–induced phosphorylation of the known ATM targets: ATM itself, structural maintenance of chromosomes 1 (SMC1), and Nijmegen breakage syndrome 1 (Nbs1; supplemental Figure 2). Pharmacologic inhibition of ATM was performed using the specific ATM inhibitor, KU-55 933 (AstraZeneca), at the dose of 5μM, shown to fully inhibit ATM kinase activity.[39]

Induction of primary CLL cell proliferation using CD40L/IL-4

Primary CLL leukemia cells obtained from the peripheral blood were typically arrested at gap 1/gap 0 (G1/G0) of the cell cycle. To stimulate and sustain proliferation of these cells, we compared 5 different mitogenic stimuli (see supplemental Figure 3) and found the CD40L/IL-4 culture system the most effective and reproducible. Briefly, after adherence of irradiated (50 Gy) CD40L-expressing murine fibroblasts at 3×10^5 cells/well, 1-1.5 $\times 10^6$ primary CLL cells were seeded into each well with 10 ng/mL IL-4 (R&D Systems) in a total volume of 2 mL RPMI containing 10% fetal calf serum (Sigma-Aldrich/PAA Laboratories) and incubated at 37°C for 3-4 days. At this point, survival assays were initiated. As bromodeoxyuridine (BrdU) staining revealed that CLL proliferation could only be sustained for 7-11 days in culture (supplemental Figure 3), primary CLL cells initiated to cycle over 3-4 days were then treated with 0-10μM olaparib (AstraZeneca) for an additional 7 days. For consistency, therefore, in all survival assays, all cell types were exposed to olaparib for only 7 days.

Isolation and culture of normal B and T cells

B and T cells were isolated from the blood of healthy donors using RosetteSep Human B-cell and T-cell Enrichment Cocktails (StemCell Technologies) according to the manufacturer's instructions. Cycling of normal B cells at a concentration of 1×10^6 cells/mL was induced as for primary CLL cells. T cells were cultured at a concentration of 1×10^6 cells/mL in RPMI containing 10% fetal calf serum with 100 IU/mL interleukin 2 (IL-2; R&D Systems).

Cell survival assays

Suspensions of lymphoid cells were exposed to increasing concentrations of olaparib for up to 7 days in triplicate experiments and counted 3 times using a hemocytometer; the surviving fraction was then calculated. In experiments using a single olaparib dose, 3μM was used irrespective of cell type, as this produced a survival response on the second part of the curve beyond the initial sharp reduction and ensured a maximal differential between normal and ATM-deficient cells. It also reflected the maximum clinically achievable dose, making the cellular effects at this dose clinically important.

Western blotting

Western blotting was performed as described[12] with the following antibodies: rabbit anti-poly(ADP-ribose) (pADPr; Calbiochem); mouse anti-PARP1 (Enzo Life Sciences); rabbit anti–phospho-ATM S1981 (Rockland Immunochemicals); mouse 11G12 anti-ATM;[12] rabbit anti–phospho-SMC1 S966 and anti-SMC1, both from Bethyl Laboratories; rabbit anti–phospho-Nbs1 S343 and anti-Nbs1, both from Abcam; mouse anti–β-actin (Sigma-Aldrich); sheep anti-p53 (D. Lane, University of Dundee, Scotland); rabbit anti-p21 (Santa Cruz Biotechnology); and rabbit anti–caspase 7 and anti–caspase 3 from Cell Signaling Technology.

BrdU staining of proliferating cells and FACS analysis

Cells were treated with 100μM BrdU (Sigma-Aldrich) for 24 hours, fixed in ethanol, treated with 2M HCl/0.1 mg/mL pepsin (VWR/Sigma-Aldrich), labeled with anti-BrdU monoclonal antibody and resuspended in 25 μg/mL propidium iodide containing 0.1 mg/mL RNase A (Sigma-Aldrich) before analysis using a Coulter Epics XL-MCL flow cytometer (Beckman Coulter).

Annexin V apoptosis assay

Apoptosis was assayed using an annexin V apoptosis kit (Becton Dickinson) according to the manufacturer's instructions and analyzed using a Coulter Epics XL-MCL flow cytometer. At least 40 000 events were scored for each condition.

Immunofluorescence

Cells were fixed to poly-L lysine–coated slides, treated with methanol (Sigma-Aldrich), and stained with the following antibodies at room temperature: For DNA damage and repair analyses, they were stained with mouse monoclonal anti-γH2AX (Millipore) and rabbit anti-RAD51 (Santa Cruz Biotechnology); for mitotic catastrophe analysis, they were stained with goat anti–Lamin B (Santa Cruz Biotechnology) and rabbit anti–phospho-Histone H3 serine-10 (Cell Signaling). After staining, they were

treated with secondary antibodies anti–mouse immunoglobulin G (IgG [Alexa Fluor 594]) and anti–rabbit (Alexa Fluor 488; Invitrogen). Slides were mounted in Vectorshield with DAPI (4,6 diamidino-2-phenylindole; Vector Laboratories). Analysis was performed using a Nikon Eclipse E600 fluorescence microscope and Velocity Version 4.1.0 software (Improvision).

Murine xenograft model

Animals were treated in accordance with United Kingdom Home Office guidelines, Schedule 1. For all experiments, tumor cell engraftment in the bone marrow and spleen before initiation of olaparib treatment was confirmed both by FACS analysis of human anti-CD45 (eBioscience)– and murine anti-CD45 (BD Pharmingen)–stained cells and by immunohistochemistry using anti–human CD5 (Leica Microsystems), anti–human Pax5 (Thermo Scientific), and anti–human Ki-67 (Dako) antibodies.

For assessment of MCL tumor load in murine primary lymphoid organs, sublethally irradiated nonobese diabetic/severe combined immunodeficient (NOD/SCID) mice (aged 5 weeks) were intravenously injected with 3×10^6 Granta-519 cells. Fourteen days after injection, animals received either 50 mg/kg/d olaparib (n = 12) or vehicle, 10% (wt/vol) 2-hydroxypropyl-β-cyclodextrin (Sigma-Aldrich; n = 11), via intraperitoneal injection, daily for 14 days. Mice were culled at day 30-36, and tumor load in the bone marrow and spleen was assessed by FACS analysis of human CD45+ cells.

To compare tumor size and survival between treated and untreated animals, subcutaneous tumors were initiated by injection of 3×10^6 Granta-519 cells. Tumors were allowed to grow for 5 days before initiation of treatment with 100 mg/kg/d olaparib (tumor size, n = 15; survival, n = 10) or vehicle alone (tumor size, n = 20; survival, n = 10) via oral gavage for no more than 28 days. Tumor volume was measured manually using a calliper 3× per week. Mice were killed upon signs of illness or when tumors reached > 1250 mm.[3]

Any mice that died early in the experiments due to graft-unrelated causes were excluded from the experiments.

Combination olaparib/cytotoxic treatment

Granta-519 cells seeded in triplicate at 1×10^5 cells/mL in a 200μL volume were pretreated with olaparib (dose range 0-10μM) for 2 days. Subsequently, increasing doses of 4-hydroxycyclophosphamide (4HC; 0-0.25μM; NIOMECH), fludarabine (0-0.5μM), valproic acid (VPA; 0-10mM), bendamustine (0-12.5μM; Sigma-Aldrich), and IR (0-5 Gy) were added to the olaparib-containing culture for an additional 5 days. This time frame enabled consistency in the duration of olaparib treatment (7 days total) and allowed sufficient time for the cytotoxic effects of the conventional agents to occur before calculation of the surviving fraction of cells. Cell viability was measured using the CellTiter-Glo luminescent cell viability assay (Promega) according to the manufacturer's instructions. Luminescence was quantified using a Wallac Victor2 1420 multilabel counter (Perkin Elmer). Synergism was determined using Calcusyn Version 2.1 for Windows software (Biosoft).

Statistical analysis

In vitro data were analyzed using 2-tailed *t* tests, in vivo tumor load data by the nonparametric Mann-Whitney U test, tumor size data by 2-way analysis of variance, and xenograft survival data by the log rank (Mantel-Cox) test. Data are presented as mean ± SEM.

Results

Olaparib selectively targets *ATM* mutant lymphoid cells, including proliferating primary CLL cells

PARP1 activity is associated with the synthesis of poly(ADP-ribose) (pADPr), which modifies a number of proteins including PARP1 itself.[32] We used immunoblotting to assess the impact of olaparib on pADPr levels as an indicator of inhibition of PARP activity. The analysis indicated comparable dose-dependent inhibition of PARP activity by olaparib in both *ATM*-wildtype and *ATM*-null LCLs and primary CLL cells with significant inhibition consistently achieved from 0.5μM olaparib (supplemental Figure 4A-B). Inhibition continued at a lesser rate with increasing doses of olaparib. We then tested the sensitivity of a range of lymphoid cells with and without *ATM* inactivation to the PARP inhibitor, olaparib, at the concentrations capable of inactivating PARP activity in lymphoid cells. These included 10 LCLs (5 control and 5 derived from ataxia telangiectasia patients; Figure 1A) and 2 MCL cells lines (*ATM* mutant Granta-519 and *ATM* wildtype JVM-2; Figure 1B). In addition, we tested 19 primary CLLs (10 *ATM* mutant and

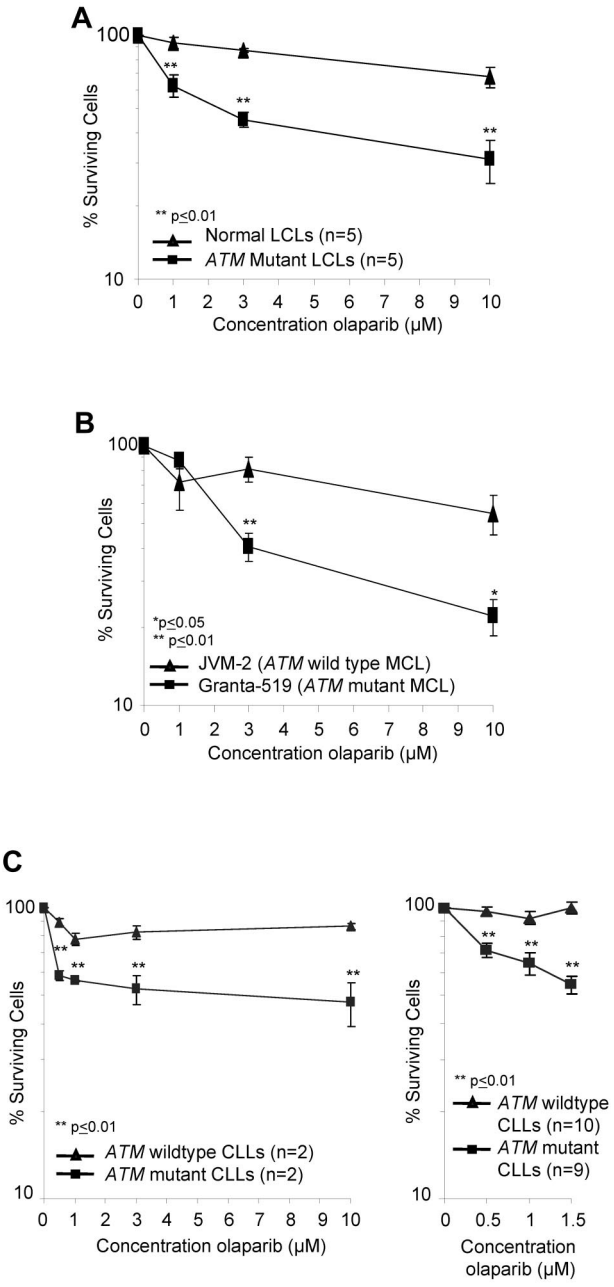

Figure 1. ATM mutant lymphoid cells are sensitive to olaparib. Effect of increasing doses of olaparib after 7 days exposure on the percentage of surviving cells (logarithmic scale) in *ATM* null and *ATM* wild-type LCLs (A), MCL cell lines (B), and proliferating primary CLL cells (C) over a broad range of doses (left) and at lower doses in an expanded cohort (right).

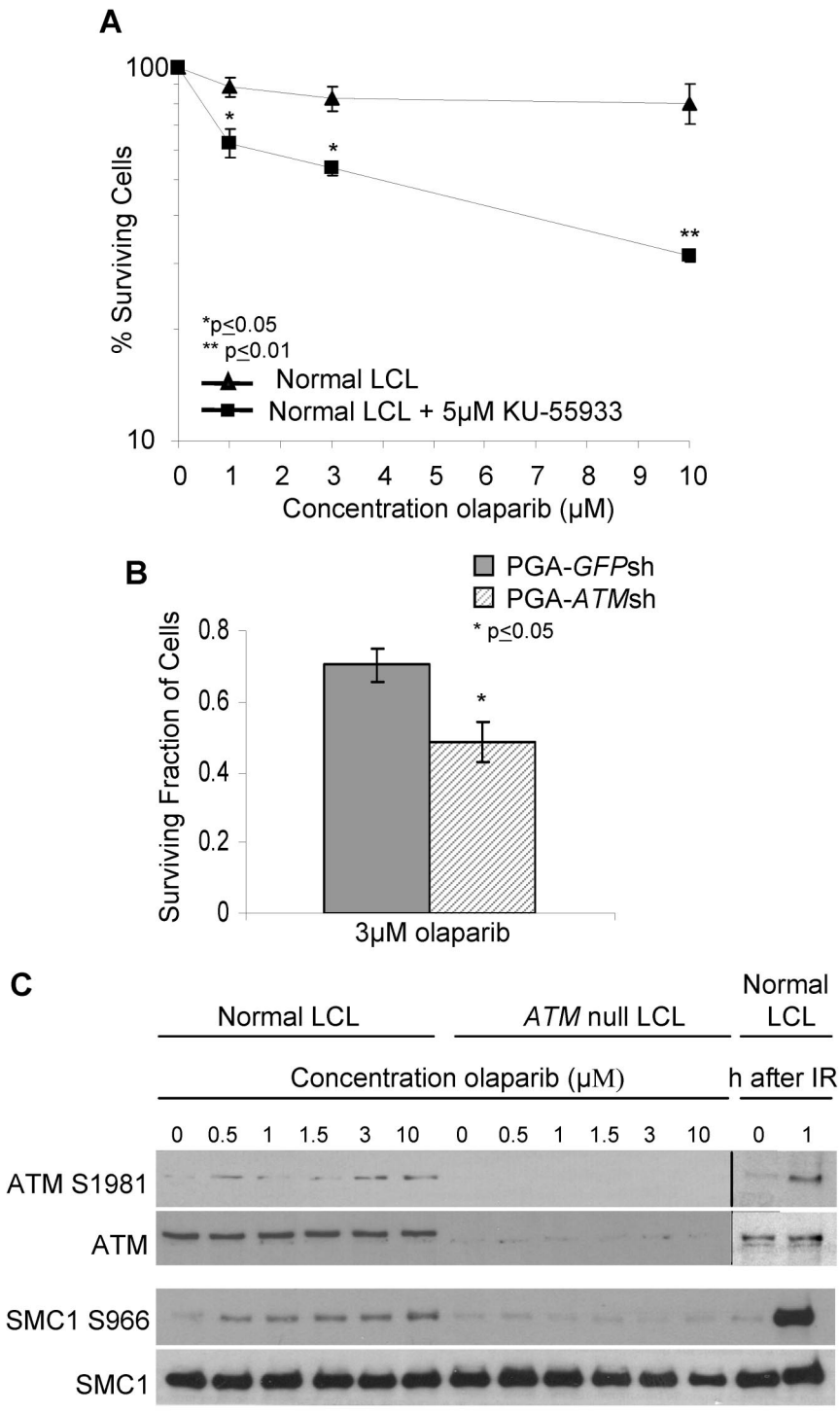

Figure 2. The cytotoxic response to olaparib is ATM-specific. Effect of increasing doses of olaparib after 7 days exposure on survival of control LCL cells treated with 5μM of the ATM inhibitor, KU-55 933 (A) and PGA cells without (*GFPsh*) and (B) with (*ATM*sh) *ATM* knockdown. (C) Immunoblotting shows olaparib-induced dose-dependent phosphorylation of ATM-dependent targets in normal cells. IR provides a positive control.

9 *ATM* wild type), which were first induced to proliferate in vitro by coculture with irradiated CD40L–expressing murine fibroblasts and IL-4 for 4 days before exposure to the drug (Figure 1C). In all lymphoid cell types tested, olaparib exposure induced greater dose-dependent reductions in the number of cells with *ATM* inactivation compared with those harboring functional ATM (Figure 1A-C). LCLs with no functional ATM revealed significant differential sensitivity to 1μM olaparib, the lowest tested dose associated with inhibition of PARP1 activity in this cell type, compared with control LCLs (Figure 1A; supplemental Figure 4A). The *ATM* mutant Granta-519 MCL cells were significantly more sensitive to olaparib at 3μM compared with JVM-2 MCL cells with ATM function (Figure 1B). Furthermore, ATM deficient–cycling CLL tumor cells, irrespective of the type of *ATM* mutation and mode of *ATM* inactivation, revealed a highly significant differential sensitivity to olaparib even at submicromolar doses of 0.5μM olaparib compared with *ATM* wild type primary tumor cells (Figure 1C). In *ATM* null CLL cells, the most prominent killing occurred between 0 and 0.5μM olaparib, consistent with the major inhibition of pADP ribose formation at 0.5μM observed by Western blot

(supplemental Figure 4B). Normal proliferating B and T cells were not sensitive to olaparib at the same doses (supplemental Figure 5).

Sensitivity to olaparib is mediated by absence of ATM activity and by cell proliferation

To determine whether sensitivity to olaparib was a consequence of specific *ATM* inactivation, we first used the small molecule ATM inhibitor, KU-55 933, to inhibit ATM activity in a normal LCL. KU-55 933 (5μM) caused complete inhibition of ATM activity (not shown) and significant sensitization of the LCL cells at a dose of 1μM olaparib (Figure 2A). Next, we down-regulated *ATM* gene expression by shRNA in the CLL cell line, PGA. *ATM* knockdown at the time of experiment was confirmed by immunoblot assessment of ATM-dependent DNA damage responses (supplemental Figure 2). We then compared the sensitivity of the isogenic cell lines pairs (PGA-*ATM*sh and PGA-*GFP*sh) to 3μM olaparib and observed significant differential sensitivity of cells with *ATM* knockdown (Figure 2B). The effects of both chemical ATM inhibition and *ATM* knockdown in sensitizing cells to 3μM olaparib measured over a relatively short period of time were significant. This most likely relates to the biologic function of ATM, which unlike BRCA2, is not a principle component of HR repair. Nonetheless, immunoblot analysis revealed that in *ATM* wildtype LCLs, but not ATM null LCLs, phosphorylation of the ATM-dependent targets ATM S1981 and SMC1 S966 was induced in a dose-dependent manner by olaparib (Figure 2C). This was consistent with PARP inhibition causing accumulation of DNA DSB, as well as the cellular response being impaired in the absence of functional ATM. Collectively, these data confirm that ATM is required for the normal cellular response to PARP inhibition and that this response is defective in lymphoid cells with ATM deficiency, resulting in sensitivity to olaparib.

Interestingly, we did not observe any differential effect of olaparib on primary *ATM* mutant CLL cells that had not been stimulated to proliferate in vitro (supplemental Figure 6), leading us to assume that olaparib preferentially targeted cells that were cycling. This was consistent with the requirement for replication during the conversion of SSBs to DSBs in the absence of PARP activity. Consequently, we assessed the sensitivity of *ATM* mutant Granta-519 cells staining positive for BrdU, which incorporates during DNA replication, after 7 days exposure to olaparib. We observed a dose-dependent decrease in the fraction of BrdU-stained cells after treatment with olaparib (Figure 3A). Furthermore, comparing 2 representative proliferating primary CLL tumors, we observed a similar trend in the percentage of BrdU-stained cells in the *ATM*-mutant but not *ATM*-wildtype CLL cells after olaparib treatment (not shown). Our findings indicate that the PARP inhibitor, olaparib, specifically targets cells that are actively cycling and exhibiting ATM dysfunction.

Given the targeting by olaparib of proliferating cells with *ATM* inactivation, we reasoned that the impact of the drug would be cumulative over longer exposure periods as a result of more cells going through 1 or more cell cycles. After treatment with olaparib for 7 days in vitro, Granta-519, PGA-*ATM*sh, and PGA-*GFP*sh cells were reseeded at a low number into new cultures with or without olaparib. Notably, the *ATM* null Granta-519 and PGA-*ATM*sh cells continuously treated with olaparib maintained complete suppression of proliferation over the additional 2 weeks of exposure, whereas PGA-*GFP*sh cells showed no such response (Figure 3B).

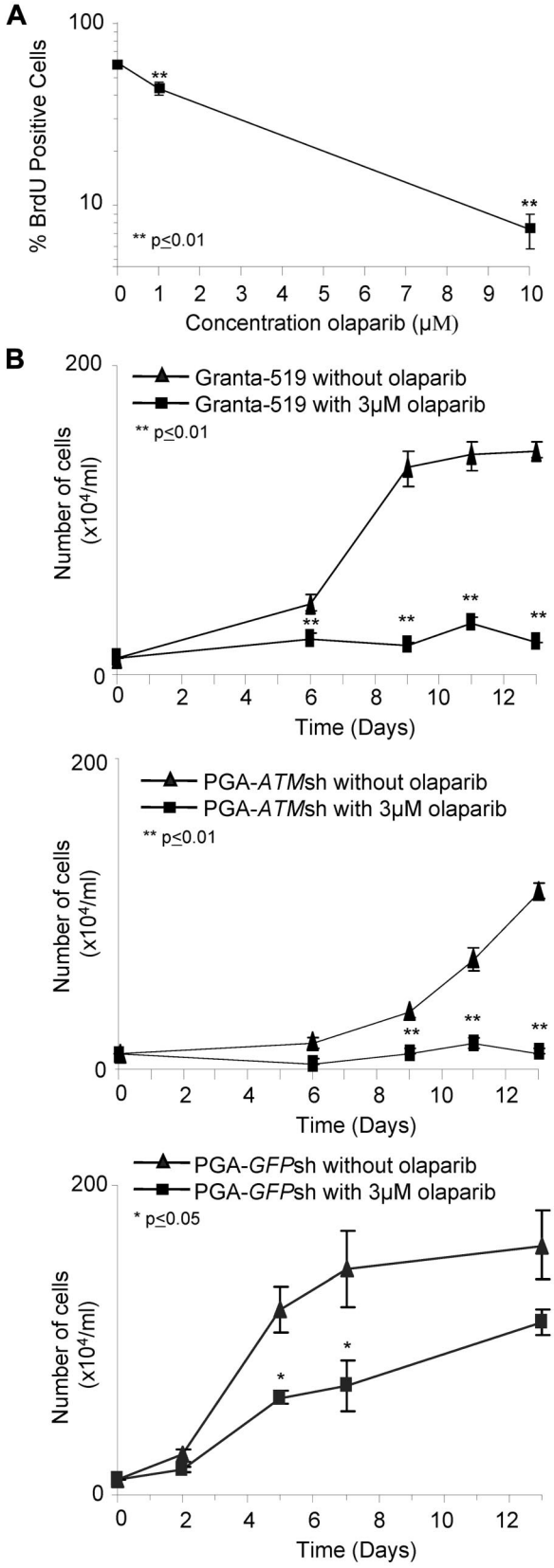

Figure 3. Olaparib targets proliferating lymphoid cells. (A) Percentage of BrdU-positive cells significantly decreases 7 days after exposure to increasing doses of olaparib in Granta-519 cells. (B) Effect of continued olaparib exposure on proliferation of ATM null cells. After 7 days exposure to 3μM olaparib, Granta519 (top), PGA-*ATM*sh (middle), and PGA-*GFP*sh (bottom), cells were reseeded at a low number and then continuously exposed to either 0μM or 3μM olaparib for an additional 2 weeks.

Olaparib sensitivity of ATM dysfunctional cells is related to the accumulation of DNA damage and is apoptosis independent

The molecular basis for olaparib activity in *ATM* deficient cells was presumed to occur by exacerbating the existing DNA DSB repair defect. We used immunofluorescence to assess olaparib-mediated DNA damage measured by γH2AX foci, a marker of DNA DSBs, and by activation of HR repair (Rad51 foci). Although rapid damage-induced formation of γH2AX foci is compromised in *ATM* null cells,[3] their persistence during prolonged PARP inhibition reflects unrepaired DSBs. We found that compared with proliferating primary CLL cells with wildtype *ATM*, those harboring *ATM* mutations exhibited significantly elevated γH2AX and RAD51 foci after 7 days exposure to 3μM olaparib (Figure 4A). This demonstrated that olaparib and ATM dysfunction cooperate in compromising DNA DSB repair leading to persistence of DNA damage and retention of repair foci. Sensitivity of *ATM*-deficient cells to olaparib could not be attributed to apoptosis-mediated cell death, as FACS analysis of annexin V/PI staining revealed an absence of apoptosis in CLL cells undergoing olaparib-induced killing (supplemental Figure 7A). This observation was corroborated, first, by the absence of stabilization of the p53 protein, its downstream target, the p21 protein, and absence of cleavage and activation of the effector caspase 3 (supplemental Figure 7B) and, second, by failure of the pan-caspase inhibitor Z-VAD-fmk to alter olaparib sensitivity (supplemental Figure 7C).

In the absence of apoptosis after olaparib treatment, we investigated the possibility of another mechanism of cell death, mitotic catastrophe, using immunofluorescence-based morphologic analysis. Mitotic catastrophe occurs when cells undergo aberrant mitosis in the presence of unrepaired DNA damage, resulting in the formation of multimicronucleated cells featuring damaged chromosomes.[40,41] Cells undergoing normal mitosis stain positive for H3 ser-10 phosphorylation yet lose integrity of the nuclear envelope, indicated by absence of lamin B1 staining. In contrast, cells undergoing mitotic catastrophe do not stain for H3 ser-10 phosphorylation but retain the nuclear envelope (and lamin B staining) due to failed cytokinesis (Figure 4B). These cells contain multiple micronuclei and are distinguishable from the nuclear blebbing of apoptotic cells, which lose integrity of the nuclear envelope. After olaparib exposure, we observed a significant elevation in the number of *ATM* mutant cells undergoing mitotic catastrophe compared with *ATM* wild-type, proliferating primary CLL cells (Figure 4C).

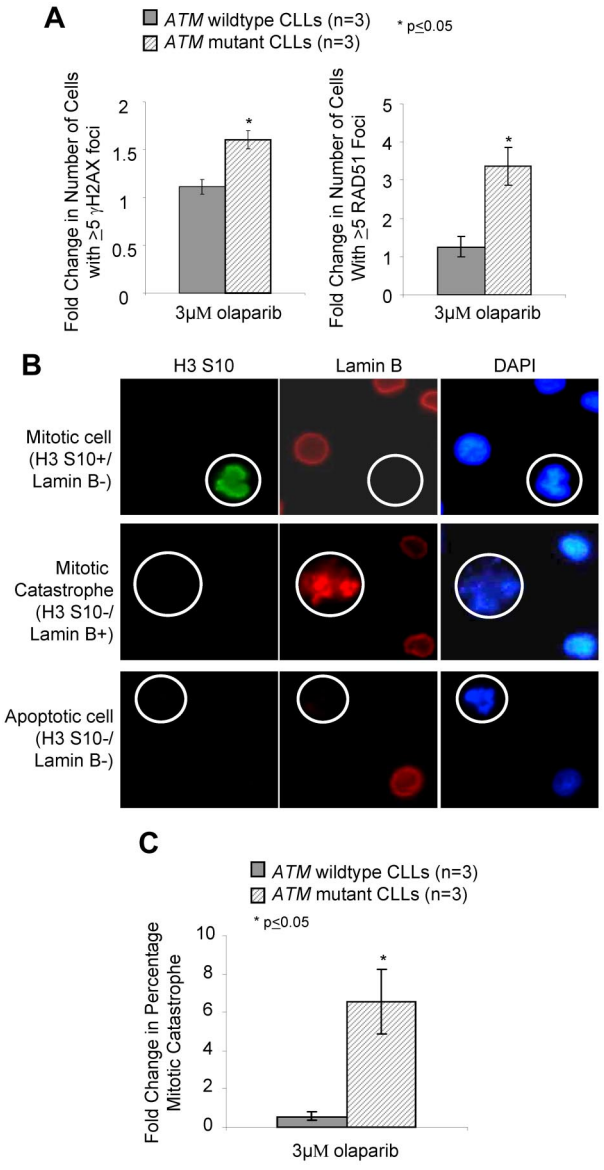

Figure 4. Olaparib induces DNA damage and mitotic catastrophe in *ATM* mutant lymphoid cells. (A) Induction of γH2AX (left) and RAD51 (right) foci after 7 days exposure to 3μM olaparib measured by immunofluorescence. (B) Differential immunofluorescent staining of cells undergoing normal mitosis (positive for H3 ser-10 phosphorylation and negative for Lamin B), mitotic catastrophe (negative for H3 serine-10 and positive for Lamin B), and apoptosis (negative for both H3 serine-10 and Lamin B), shown at original magnification ×500. (C) Induction of mitotic catastrophe determined by immunofluorescence-based morphologic analysis after 72 hours exposure to 3μM olaparib.

ATM-mutant lymphoid tumor cells are sensitive to olaparib in vivo

To investigate the in vivo impact of olaparib, we generated murine xenograft models of the *ATM* mutant MCL cell line, Granta-519. To determine whether infiltration and engraftment of the tumor cell line had already taken place before initiation of olaparib treatment in the different animal cohorts, 3 representative mice from each cohort were analyzed on the day that treatment was to begin (14 days after intravenous or 5 days after subcutaneous injection of cells). The presence of tumor cells at the level of at least 1% of all cells, which is considered to be engraftment, was observed by FACS analysis in the bone marrow and spleen both at 5 days (subcutaneous) and 14 days (intravenous) after injection (Figure 5A). Furthermore, using immunocytochemistry and anti–human CD5, Pax-5, and Ki-67 antibodies, we confirmed significant infiltration of proliferating human B-lymphoid tumor cells in both the spleen and bone marrow at both time points before treatment initiation (Figure 5A).

Subsequently, the degree of tumor load was compared in the lymphoid organs of 23 NOD/SCID Granta-519 cell–injected mice 5 weeks after intravenous injection of cells and 14 days after treatment with olaparib. However, early in the experiment, 7 mice died of graft-unrelated causes, leaving 16 mice, which were treated with either olaparib (n = 8) or vehicle alone (n = 8). Analysis of the percentage of human CD45 staining by FACS analysis (Figure 5B) revealed a significant reduction in the percentage of Granta-519 cells in the bone marrow and a trend toward reduced tumor cell load in the spleen of mice treated with olaparib compared with those receiving vehicle alone (Figure 5B).

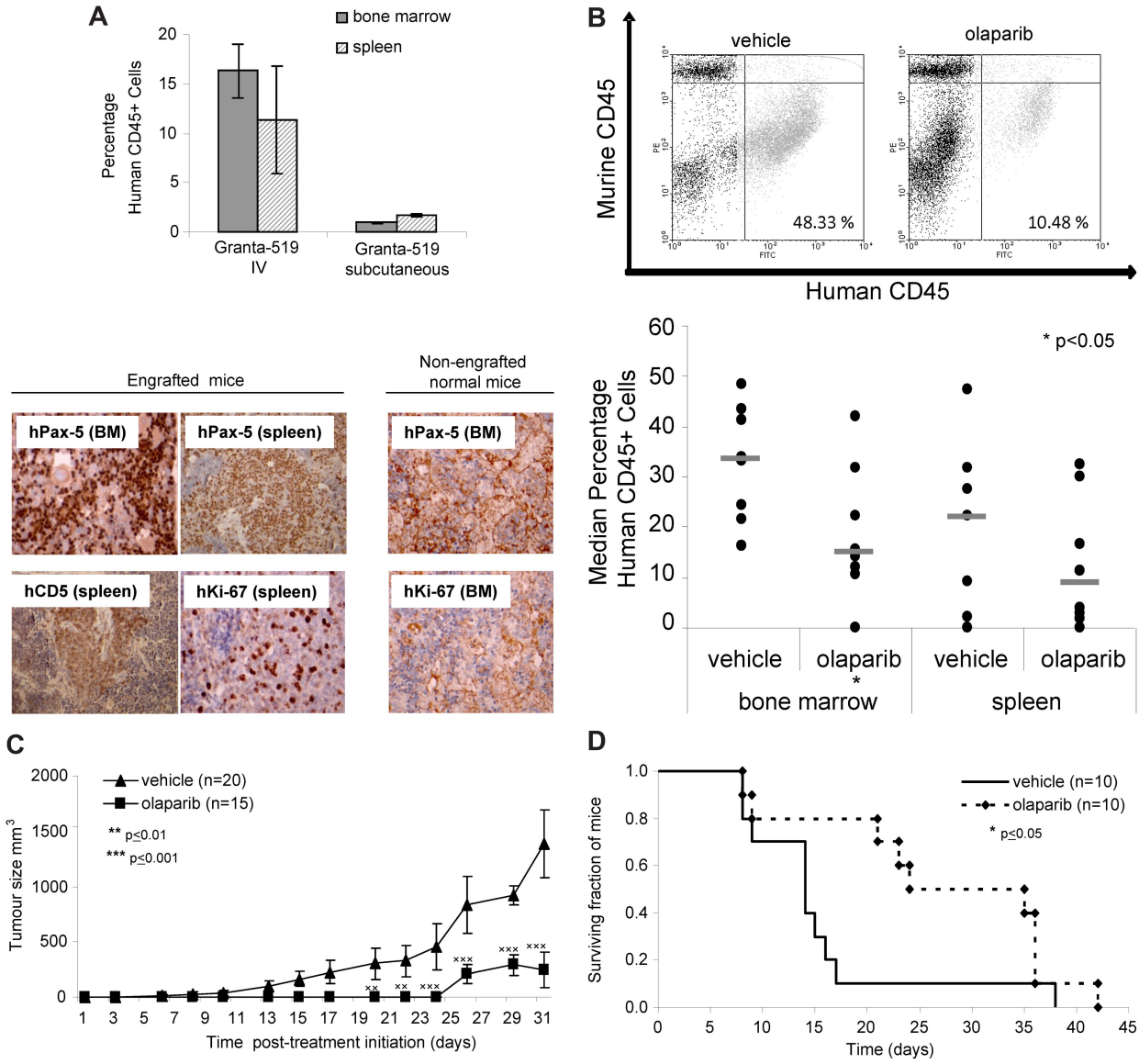

Figure 5. Olaparib impedes growth of *ATM* mutant tumor cells in vivo and lengthens survival in a Granta-519 murine xenograft model. (A) Engraftment of a human tumor cell line in bone marrow and spleen of representative mice before treatment. Engraftment was demonstrated 14 days after intravenous injection or 5 days after subcutaneous injection of 3×10^6 Granta-519 cells/animal by FACS assessment of the percentage of human CD45+cells (top) and by immunohistochemistry using anti–human antibodies for B-cell lineage (CD5 and Pax5) and proliferating cells (Ki-67; bottom) in the spleen and bone marrow of mice (shown either at original magnification ×20 or ×40). Brown color indicates positive immunostaining. Organs from non-engrafted mice did not show nuclear staining for either hKi-67 or hPax5. (B) Effect of olaparib exposure on tumor burden in Granta-519–engrafted NOD/SCID mice. Representative FACS dot plots showing percentage of human CD45+ cells in murine bone marrow after treatment with olaparib or vehicle alone (top) and median percentage of human CD45+ cells in the bone marrow and spleen of mice intravenously injected with Granta-519 cells after 5 weeks treatment with olaparib (n = 8) or vehicle alone (n = 8; bottom). (C) Effect of olaparib treatment on size of subcutaneous tumors generated by localized Granta-519 injection (n = 15) compared with vehicle alone (n = 20). (D) Impact of olaparib treatment on overall survival of mice engrafted with Granta-519 cells (n = 10) compared with vehicle alone (n = 10).

We next assessed the effect of olaparib on the growth of subcutaneous tumors generated by the localized injection of *ATM* mutant Granta-519 cells into mice and found a significant positive correlation between olaparib treatment and reduced tumor size (Figure 5C). Finally, the overall survival of mice engrafted with Granta-519 cells was significantly increased by olaparib treatment compared with vehicle alone (Figure 5D).

Collectively, these data provide convincing evidence that 4 weeks of continuous intraperitoneal or oral treatment with 50 or 100 mg/kg olaparib significantly impedes the growth of *ATM* mutant tumor cells and consequently lengthens the survival of animals harboring these tumors.

We conclude that *ATM* mutant malignant lymphoid cells show differential sensitivity to PARP inhibition both in vitro and in vivo.

Olaparib sensitizes ATM mutant cells to conventional cytotoxic agents

Finally, to address the ability of PARP inhibition to increase the effect of standard CLL treatments as well as other chemotherapy agents, we tested the ability of olaparib to sensitize *ATM* mutant cells to the purine analogue fludarabine, the alkylating agents 4HC and bendamustine, the histone deacetylase inhibitor VPA, and IR (supplemental Table 2; Figure 6A). When treated with the agents

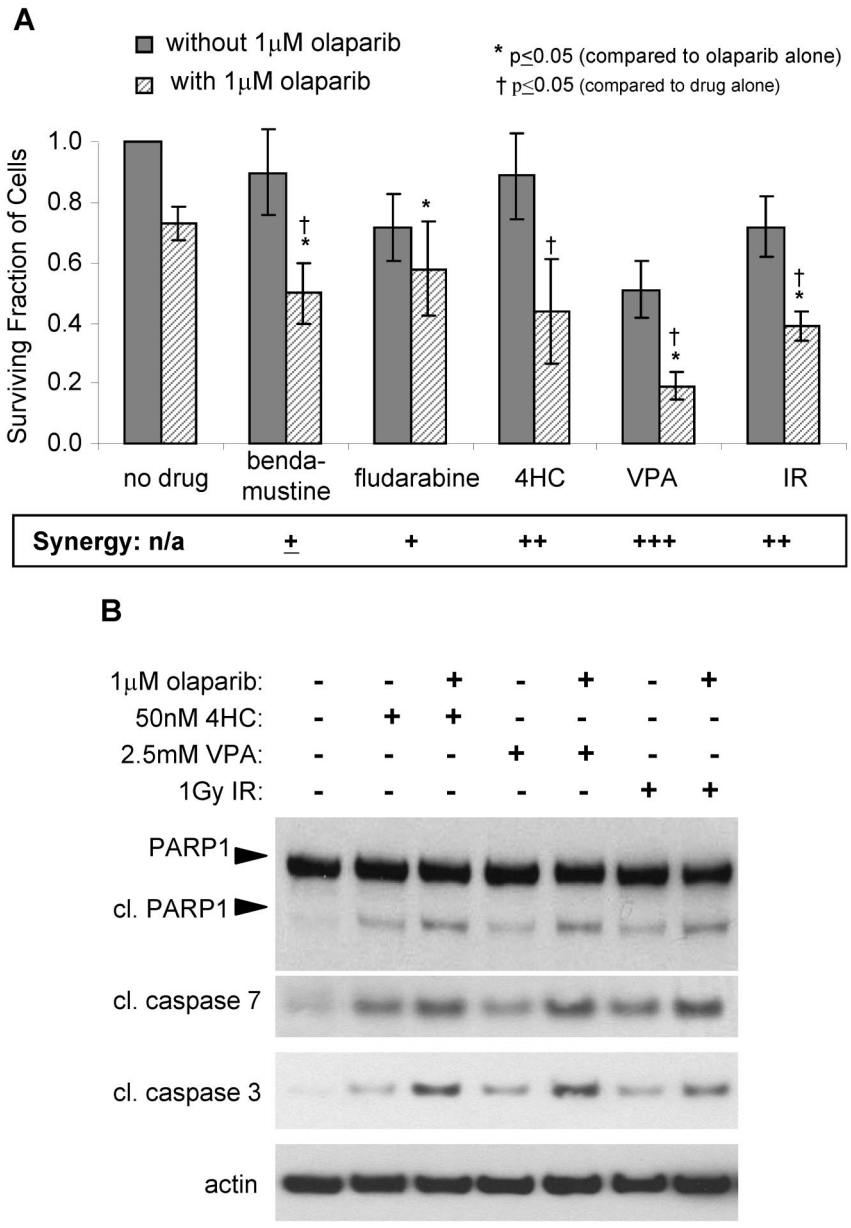

Figure 6. Pretreatment with olaparib sensitizes ATM null cells to cytotoxic agents. (A) Effect of 1μM olaparib on killing by 12.5μM bendamustine, 0.1μM fludarabine, 0.1μM 4HC, 5mM VPA, and 1 Gy IR in *ATM* mutant Granta-519 cells. Synergistic effects (see supplemental Table 2) for the given doses are shown below the graph (+++ synergism; ++ moderate synergism; + slight synergism; ± nearly additive). (B) Western blot analysis of Granta-519 cells showing an increased cleavage of PARP1, caspase 7, and caspase 3 after combined olaparib plus 4HC, VPA, or IR treatment compared with treatment with 4HC, VPA, or IR alone. Actin shows equal loading.

alone, Granta-519 cells were resistant to bendamustine and 4HC, yet were sensitive to VPA. Olaparib pretreatment was able to significantly sensitize cells to all the agents tested (Figure 6A). The greatest synergism was observed between olaparib and VPA, whereas olaparib and IR revealed only moderate synergism (supplemental Table 2). The effect of 4HC and olaparib was largely additive (supplemental Table 2), although moderate synergism was observed at the 4HC dose of 0.1μM (Figure 6A). Finally, the impact of olaparib on fludarabine and bendamustine cytotoxicity was generally additive, although synergistic activity could be detected at some doses of fludarabine (supplemental Table 2). Western blot analysis demonstrated enhanced cleavage of PARP1 and caspases 3 and 7 when Granta-519 cells were exposed to either 4HC, VPA, or IR in combination with 1μM olaparib (Figure 6B), indicating that drug-induced apoptosis was increased in the presence of olaparib.

Overall, these data indicate that olaparib is able to sensitize *ATM* null cells in vitro to conventional chemotherapy agents used for the treatment of leukemias.

Discussion

ATM mutation represents the single most frequent genetic alteration in CLL, as well as in the more rare, aggressive lymphoproliferative disorders T-PLL and MCL.[12-17] The nature of chemoresistant *ATM* mutant leukemia[20,21] is reflected at the biologic level by an apoptotic defect in response to DNA damaging agents.[42,43] Importantly, and distinct from *TP53* mutant cells, which are also apoptosis resistant, the DNA damage response defect of *ATM* mutant lymphoid cells extends to multiple pathways, demonstrated by impaired phosphorylation of downstream protein targets, such

as SMC1 and Nbs1, and DNA repair.[20,42,43] Thus, manipulating the DNA damage response may enable sensitization of *ATM* mutant lymphoid cells to DNA damage despite the presence of an apoptotic defect.

In the current study, we have demonstrated that the PARP inhibitor olaparib is able to enhance a pre-existing DNA repair defect in *ATM* mutant lymphoid tumor cells, leading to the accumulation of unrepaired DNA DSBs and apoptotic-independent cell death, which involved the process of mitotic catastrophe. The growth of *ATM* mutant Granta-519 tumor cells in a NOD/SCID xenograft model was significantly impaired in the presence of olaparib, both in primary lymphoid organs as well as in subcutaneous tumors. Furthermore, the overall survival of the Granta-519–engrafted NOS/SCID mice was significantly increased by olaparib treatment compared with mice receiving vehicle alone. Overall, our findings indicate that olaparib impedes the growth of *ATM* mutant cells in vitro and in vivo by instigating the accumulation of intolerable levels of DNA damage in cycling cells.

The observed effect of olaparib in *ATM* mutant lymphoid cells as a result of off-target effects has to be formally considered. Off-target effects are unlikely, as, first, we observed a tumor-specific effect in *ATM* null lymphoid tumor cells with olaparib, and, second, olaparib treatment produced a cytotoxic effect, which led to both the accumulation of DNA damage and inhibition of PARP activity in primary CLL cells at similar submicromolar/micromolar doses. Thus, the activity of olaparib was clearly dependent on ATM dysfunction and represents a novel targeted therapy for *ATM* mutant lymphoid tumors.

These observations suggest that primary *ATM* mutant leukemias may be predicted to show a differential sensitivity to PARP inhibition–mediated killing in vivo in a manner dependent on their highly proliferative status and, importantly, independent of p53-mediated apoptosis. Olaparib, here, targets only proliferating cells with ATM dysfunction, consistent with a cytotoxic mechanism involving the conversion of SSBs into DSBs during DNA replication that cannot be repaired efficiently in cells with a HR repair defect. PARP inhibition did not lead to the same degree of cytotoxicity of ATM deficient tumor cells as *BRCA* mutant cells,[29,30] because the major role of ATM is in sensing the damage that is subsequently repaired by HR repair in which Rad51, BRCA2 and BRCA1 proteins play a major role. A mechanism that is independent of an HR defect and allows some *ATM* mutant cells to survive in the presence of olaparib could potentially account for the lesser effect. However, this possibility is less likely given that several other proteins in the HR pathway, when inactivated, also result in cellular sensitivity to olaparib comparable in scale with ATM null cells.[34] The response of *ATM* mutant lymphoid tumor cells to PARP inhibition is, therefore, comparable to, although not the same as, the scenario previously described for *BRCA1/2* mutant breast carcinoma cells,[29,30] which has resulted in Phase I and ongoing Phase II clinical trials with orally administrated olaparib, providing evidence that this agent is well tolerated and exhibits clinical potency.[36,44] Thus, the clear differential sensitivity of *ATM* mutant lymphoid cells to submicromolar concentrations of olaparib and the necessity to improve treatment for chemoresistant *ATM* mutant lymphoid tumors makes olaparib a compelling candidate for trials in these malignancies. Indeed, progressive tumors with especially active proliferation centers[45,46] may provide the ideal cellular scenario for targeting by olaparib with the aim of at least delaying disease progression.

There is a possibility that different *ATM* mutant lymphoid tumors will exhibit differential sensitivity to olaparib, depending on the type of *ATM* mutation(s) and, consequently, the degree of residual ATM activity. In the current study, we did not observe a difference in response to olaparib between primary CLL tumors with either a single or 2 identified *ATM* mutations. This may not be surprising, given that *ATM* mutant tumors were initially selected on the basis of their defective response to DNA damage and therefore loss of ATM kinase activity. It is also possible that some single mutant alleles might act in a dominant negative manner. As we have shown in the context of CLL, loss of a single *ATM* allele by 11q deletion does not affect ATM function,[21] and it is therefore conceivable that only 11q-deleted tumors that exhibit mutation in the remaining *ATM* allele and consequently lose ATM function will respond differentially to treatment with olaparib. Although accurate measurement of the in vivo proliferative rate of *ATM*-deficient CLL tumors is not yet available, there is data to suggest that cases of progressive disease, which are often associated with *ATM* mutations, are generally associated with increased cell turnover.[45,46] Consistent with this notion, 11qdel CLL subclones expand more rapidly in vivo after acquisition of homozygous *ATM* gene inactivation.[21] While olaparib monotherapy is an attractive proposition for treating these challenging tumors, there is also the possibility of combining olaparib with chemotherapy agents. Indeed, we have shown that addition of olaparib acts in a cooperative manner with several conventional chemotherapy agents and increases the sensitivity of ATM null lymphoid tumor cells to alkylating agents and purine anologs. Interestingly, clear synergistic activity of olaparib was observed with the histone deacetylase inhibitor, VPA. Thus, the combination of VPA and olaparib may prove to be a useful and novel clinical approach to treating chemoresistant ATM null CLLs. Finally, it remains to be determined whether, in addition to ATM inactivation, refractory CLL tumors with chromosomal instability[47] exhibit other types of HR repair defects that might render them sensitive to PARP inhibition.

Acknowledgments

We thank Claire Baker, Clemency Hawksley, the BMSU staff, and Oliver G. Best for technical support; Professor John Gordon for CD40L-expressing fibroblasts; and Anders Rosen for CLL cell lines.

This work was supported by Leukaemia Lymphoma Research UK, Cancer Research UK, and AstraZeneca.

Authorship

Contribution: V.J.W. and C.E.O. designed the work, performed experiments, interpreted the data, and wrote the manuscript; A.S. performed experiments; D.G.O., G.P., and M.J.S.D. wrote the manuscript; G.S. designed the work and wrote the manuscript; J.E.P. analyzed the data; Z.R. performed experiments; P.K. designed the work; P.A.H.M. wrote the manuscript; A.M.R.T. designed the work, interpreted the data, and wrote the manuscript; and T.S. designed the work, interpreted the data, and wrote the manuscript.

Conflict-of-interest disclosure: C.E.O. has been supported by AstraZeneca, and G.S. is an employee of AstraZeneca. The remaining authors declare no competing financial interests.

Correspondence: Tatjana Stankovic, School of Cancer Sciences, Birmingham University, Vincent Dr, Edgbaston, Birmingham, B15 2TT, United Kingdom; e-mail: t.stankovic@bham.ac.uk.

References

1. Taylor AM, Harnden DG, Arlett CF, et al. Ataxia telangiectasia: a human mutation with abnormal radiation sensitivity. *Nature.* 1975;258(5534): 427-429.
2. Jorgensen TJ, Shiloh Y. The ATM gene and the radiobiology of ataxia-telangiectasia. *Int J Radiat Biol.* 1996;69(5):527-537.
3. Lavin MF. Ataxia-telangiectasia: from a rare disorder to a paradigm for cell signalling and cancer. *Nat Rev Mol Cell Biol.* 2008;9(10):759-769.
4. Löbrich M, Jeggo PA. The impact of a negligent G2/M checkpoint on genomic instability and cancer induction. *Nat Rev Cancer.* 2007;7(11): 861-869.
5. Taylor AM, Byrd PJ. Molecular pathology of ataxia telangiectasia. *J Clin Pathol.* 2005;58(10):1009-1015.
6. Kühne M, Riballo E, Rief N, et al. A double-strand break repair defect in ATM-deficient cells contributes to radiosensitivity. *Cancer Res.* 2004;64(2): 500-508.
7. Riballo E, Kühne M, Rief N, et al. A pathway of double-strand break rejoining dependent upon ATM, Artemis, and proteins locating to gamma-H2AX foci. *Mol Cell.* 2004;16(5):715-724.
8. Maser RS, Monsen KJ, Nelms BE, et al. hMre11 and hRad50 nuclear foci are induced during the normal cellular response to DNA double-strand breaks. *Mol Cell Biol.* 1997;17(10):6087-6096.
9. Chen G, Yuan SS, Liu W, et al. Radiation-induced assembly of Rad51 and Rad52 recombination complex requires ATM and c-Abl. *J Biol Chem.* 1999;274(18):12748-12752.
10. Morrison C, Sonoda E, Takao N, et al. The controlling role of ATM in homologous recombinational repair of DNA damage. *EMBO J.* 2000; 19(3):463-471.
11. Yuan SS, Chang HL, Lee EY. Ionizing radiation-induced Rad51 nuclear focus formation is cell cycle-regulated and defective in both ATM(−/−) and c-Abl(−/−) cells. *Mutat Res.* 2003;525(1-2): 85-92.
12. Stankovic T, Weber P, Stewart G, et al. Inactivation of ataxia telangiectasia mutated gene in B-cell chronic lymphocytic leukaemia. *Lancet.* 1999;353(9146):26-29.
13. Pettitt AR, Sherrington PD, Stewart G, et al. p53 dysfunction in B-cell chronic lymphocytic leukemia: inactivation of ATM as an alternative to TP53 mutation. *Blood.* 2001;98(3):814-822.
14. Stankovic T, Stewart GS, Byrd P, et al. ATM mutations in sporadic lymphoid tumours. *Leuk Lymphoma.* 2002;43(8):1563-1571.
15. Vorechovský I, Luo L, Dyer MJ, et al. Clustering of missense mutations in the ataxia-telangiectasia gene in a sporadic T-cell leukaemia. *Nat Genet.* 1997;17(1):96-99.
16. Stilgenbauer S, Schaffner C, Litterst A, et al. Biallelic mutations in the ATM gene in T-prolymphocytic leukemia. *Nat Med.* 1997;3(10):1155-1159.
17. Schaffner C, Idler I, Stilgenbauer S, et al. Mantle cell lymphoma is characterized by inactivation of the ATM gene. *Proc Natl Acad Sci U S A.* 2000; 97(6):2773-2778.
18. Zenz T, Habe S, Denzel T, et al. Detailed analysis of p53 pathway defects in fludarabine-refractory CLL: dissecting the contribution of 17p deletion, TP53 mutation, p53-p21 dysfunction, and miR34a in a prospective clinical trial. *Blood.* 2009; 114(13):2589-2597.
19. Rossi D, Cerri M, Deambrogi C, et al. The prognostic value of TP53 mutations in chronic lymphocytic leukemia is independent of Del17p13: implications for overall survival and chemorefractoriness. *Clin Cancer Res.* 2009;15(3):995-1004.
20. Austen B, Powell JE, Alvi A, et al. Mutations in the ATM gene lead to impaired overall and treatment-free survival that is independent of IGVH mutation status in patients with B-CLL. *Blood.* 2005; 106(9):3175-3182.
21. Austen B, Skowronska A, Baker C, et al. Mutation status of the residual ATM allele is an important determinant of the cellular response to chemotherapy and survival in patients with chronic lymphocytic leukemia containing an 11q deletion. *J Clin Oncol.* 2007;25(34):5448-5457.
22. Keating MJ, Chiorazzi N, Messmer B, et al. Biology and treatment of chronic lymphocytic leukemia. *Hematology Am Soc Hematol Educ Program.* 2003;(1):153-175.
23. Grever MR, Lucas DM, Johnson AJ, et al. Novel agents and strategies for treatment of p53-defective chronic lymphocytic leukemia. *Best Pract Res Clin Haematol.* 2007;20(3):545-556.
24. Maddocks KJ, Lin TS. Update in the management of chronic lymphocytic leukaemia. *J Hematol Oncol.* 2009;2:29.
25. CLL Trialists' Collaborative Group. Chemotherapeutic options in chronic lymphocytic leukemia: a meta-analysis of the randomized trials. *J Natl Cancer Inst.* 1999;91(10):861-868.
26. Obrador-Hevia A, Fernández de Mattos S, Villalonga P, et al. Molecular biology of mantle cell lymphoma: from profiling studies to new therapeutic strategies. *Blood Rev.* 2009;23(5):205-216.
27. Dungarwalla M, Matutes E, Dearden CE. Prolymphocytic leukaemia of B- and T-cell subtype: a state-of-the-art paper. *Eur J Haematol.* 2008;80(6): 469-476.
28. Helleday T, Petermann E, Lundin C, et al. DNA repair pathways as targets for cancer therapy. *Nat Rev Cancer.* 2008;8(3):193-204.
29. Bryant HE, Schultz N, Thomas HD, et al. Specific killing of BRCA2-deficient tumours with inhibitors of poly(ADP-ribose) polymerase. *Nature.* 2005; 434(7035):913-917.
30. Farmer H, McCabe N, Lord CJ, et al. Targeting the DNA repair defect in BRCA mutant cells as a therapeutic strategy. *Nature.* 2005;434(7035): 917-921.
31. Dantzer F, Schreiber V, Niedergang C, et al. Involvement of poly(ADP-ribose) polymerase in base excision repair. *Biochimie.* 1999;81(1-2): 69-75.
32. Bryant HE, Helleday T. Poly(ADP-ribose) polymerase inhibitors as potential chemotherapeutic agents. *Biochem Soc Trans.* 2004;32(Pt6): 959-961.
33. Bryant HE, Helleday T. Inhibition of poly (ADP-ribose) polymerase activates ATM which is required for subsequent homologous recombination repair. *Nucleic Acids Res.* 2006;34(6): 1685-1691.
34. McCabe N, Turner NC, Lord CJ, et al. Deficiency in the repair of DNA damage by homologous recombination and sensitivity to poly(ADP-ribose) polymerase inhibition. *Cancer Res.* 2006;66(16): 8109-8115.
35. Menear KA, Adcock C, Barlter R, et al. 4-[3-(4-Cyclopropanecarbonylpiperazine-1-carbonyl)-4-fluorobenzyl]-2H-phthalazin-1-one: a novel bioavailable inhibitor of poly(ADP-ribose) polymerase-1. *J Med Chem.* 2008;51(20): 6581-6591.
36. Fong PC, Boss DS, Yap TA, et al. Inhibition of poly(ADP-ribose)polymerase in tumours from BRCA mutation carriers. *N Engl J Med.* 2009;361(2):123-134.
37. Lewin N, Minarovits J, Weber G, et al. Clonality and methylation status of the Epstein-Barr virus (EBV) genomes in *in vivo*-infected EBV-carrying chronic lymphocytic leukaemia (CLL) cell lines. *Int J Cancer.* 1991;48(1):62-66.
38. Biton S, Dar I, Mittelman L, et al. Nuclear ataxia-telangiectasia mutated (ATM) mediates the cellular response to DNA double strand breaks in human neuron-like cells. *J Biol Chem.* 2006; 281(25):17482-17491.
39. Hickson I, Zhao Y, Richardson CJ, et al. Identification and characterization of a novel and specific inhibitor of the ataxia-telangiectasia mutated kinase ATM. *Cancer Res.* 2004;64(24): 9152-9159.
40. Alderton GK, Joenje H, Varon R, et al. Seckel syndrome exhibits cellular features demonstrating defects in the ATR-signalling pathway. *Hum Mol Genet.* 2004;13(24):3127-3138.
41. Blank M, Lerenthal Y, Mittelman L, et al. Condensin I recruitment and uneven chromatin condensation precede mitotic cell death in response to DNA damage. *J Cell Biol.* 2006;174(2): 195-206.
42. Stankovic T, Stewart GS, Fegan C, et al. Ataxia telangiectasia mutated-deficient B-cell chronic lymphocytic leukemia occurs in pregerminal center cells and results in defective damage response and unrepaired chromosome damage. *Blood.* 2002;99(1):300-309.
43. Stankovic T, Hubank M, Cronin D, et al. Microarray analysis reveals that *TP53*- and *ATM*-mutant B-CLLs share a defect in activating proapoptotic responses after DNA damage but are distinguished by major differences in activating prosurvival responses. *Blood.* 2004;103(1):291-300.
44. Yap TA, Boss DS, Fong PC, et al. First in human phase I pharmacokinetic (PK) and pharmacodynamic (PD) study of KU-0059436 (Ku), a small molecule inhibitor of poly ADP-ribose polymerase (PARP) in cancer patients (p), including BRCA1/2 mutation carriers. *J Clin Oncol ASCO Ann Meet Proc Pt I.* 2007;25(18S):3529.
45. Messmer BT, Messmer D, Allen SL, et al. In vivo measurements document the dynamic cellular kinetics of chronic lymphocytic leukemia B cells. *J Clin Invest.* 2005;115(3):755-764.
46. Chiorazzi N, Ferrarini M. Evolving view of the in-vivo kinetics of chronic lymphocytic leukemia B cells. *Hematology Am Soc Hematol Educ Program.* 2006;(1):273-278.
47. Kujawski L, Ouillette P, Erba H, et al. Genomic complexity identifies patients with aggressive chronic lymphocytic leukaemia. *Blood.* 2008; 112(5):1993-2003.